Cell Reports
Physical Science

CellPress
OPEN ACCESS

Article

Virus blocking textile for SARS-CoV-2 using human body triboelectric energy harvesting

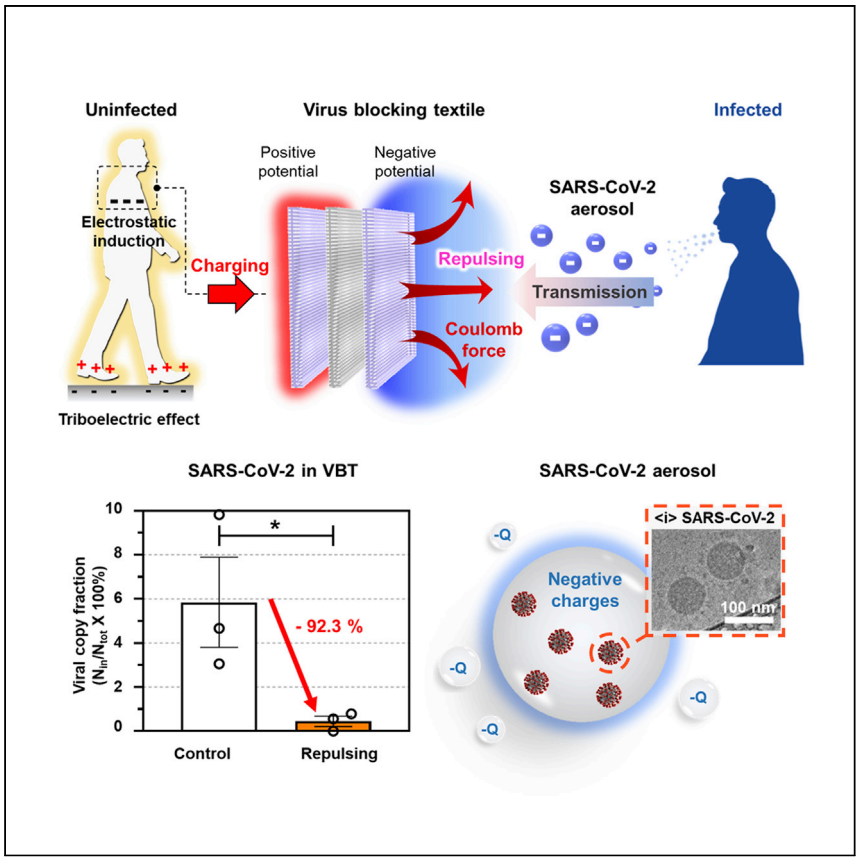

Effective mitigation technology to prevent the spread of SARS-CoV-2 is required before achieving population immunity through vaccines. Kang et al. propose a virus-blocking textile that blocks SARS-CoV-2 by 99.95% by applying repulsive Coulomb force to respiratory particles, based on sustainable powering by the human body's triboelectric energy harvesting.

Minki Kang, Na-Yoon Jang, Young-Jun Kim, ..., Byung-Ok Choi, Nam-Hyuk Cho, Sang-Woo Kim

kimsw1@skku.edu (S.-W.K.)
chonh@snu.ac.kr (N.-H.C.)
bochoi@skku.edu (B.-O.C.)

Highlights

Negative charge of SARS-CoV-2 is validated

A virus blocking textile (VBT) blocks SARS-CoV-2 using repulsive Coulomb force

The VBT is sustainably powered by a human body based on triboelectric effect

The VBT blocks SARS-CoV-2 by 99.95% at the flow rate of 0.5 m/s

Kang et al., Cell Reports Physical Science 3, 100813
April 20, 2022
https://doi.org/10.1016/j.xcrp.2022.100813

Cell Reports
Physical Science

CellPress
OPEN ACCESS

Article

Virus blocking textile for SARS-CoV-2 using human body triboelectric energy harvesting

Minki Kang,[1,10] Na-Yoon Jang,[2,3,10] Young-Jun Kim,[1,10] Hyo-Jin Ro,[2,3,10] Dabin Kim,[1] Yuri Kim,[2] Hyoung Taek Kim,[1] Hye Mi Kwon,[4] Jin-Hyun Ahn,[5] Byung-Ok Choi,[4,6,7,*] Nam-Hyuk Cho,[2,3,8,*] and Sang-Woo Kim[1,7,9,11,*]

SUMMARY

Effective mitigation technology to prevent the spread of severe acute respiratory syndrome coronavirus 2 (SARS-CoV-2) is required before achieving population immunity through vaccines. Here we demonstrate a virus-blocking textile (VBT) that repulses SARS-CoV-2 by applying repulsive Coulomb force to respiratory particles, powered by human body triboelectric energy harvesting. We show that SARS-CoV-2 has negative charges, and a human body generates high output current of which peak-to-peak value reaches 259.6 μA at most, based on triboelectric effect. Thereby, the human body can sustainably power a VBT to have negative electrical potential, and the VBT highly blocks SARS-CoV-2 by repulsion. In an acrylic chamber study, we found that the VBT blocks SARS-CoV-2 by 99.95%, and SARS-CoV-2 in the VBT is 13-fold reduced. Our work provides technology that may prevent the spread of virus based on repulsive Coulomb force and triboelectric energy harvesting.

INTRODUCTION

Since the first human case of coronavirus disease in 2019 caused by SARS-CoV-2 was reported, infection with the virus increased exponentially and rapidly spread all over the world; 72 million people were infected, and 1.6 million died in the first year.[1,2] This together with the emergence of multiple variants of SARS-CoV-2 that ranged from alpha to epsilon provoked an unprecedented demand for effective mitigation technology.[3–6] Developments of vaccines are fundamental and long-term solutions.[7,8] However, the development and massive production of enough vaccines to achieve global population immunity are projected to take several years, and reduction of efficacy of a vaccine has possibly occurred by the emergence of multiple variants. Therefore, immediate and short-term mitigation strategies are required to resist the pandemic.[9]

Wearing a face mask and medical protective clothing represent effective methods to block the transmission of SARS-CoV-2; they block respiratory aerosols (aerodynamic diameter ≤ 5 μm) or droplets (aerodynamic diameter >5 μm).[10–12] To provide a high level of protection, there are two important requirements: continuousness and high filtration efficiency. Although the efficacies of filters such as electrostatic filters,[13,14] surgical face masks,[15] and silk or cotton textiles[16] have been widely investigated globally, none of them have achieved two requirements at the same time. Although the electrostatic filters effectively capture respiratory particles by attracting them with static charges, the filtration efficiency drastically decreases by losing static charge in a few hours. Surgical face masks and silk or cotton textile continuously

[1]School of Advanced Materials Science and Engineering, Sungkyunkwan University (SKKU), Suwon 16419, Republic of Korea

[2]Department of Microbiology and Immunology, Seoul National University College of Medicine, Seoul 03080, Republic of Korea

[3]Department of Biomedical Sciences, Seoul National University College of Medicine, Seoul 03080, Republic of Korea

[4]Department of Neurology, Samsung Medical Center, Sungkyunkwan University School of Medicine, Seoul 06351, Republic of Korea

[5]Department of Microbiology, Sungkyunkwan University School of Medicine, Suwon 16419, Republic of Korea

[6]Stem Cell and Regenerative Medicine Institute, Samsung Medical Center, Seoul 06351, Republic of Korea

[7]Samsung Advanced Institute for Health Sciences & Technology (SAIHST), Sungkyunkwan University (SKKU), Seoul 06351, Republic of Korea

[8]Institute of Endemic Disease, Seoul National University Medical Research Center and Bundang Hospital, Seoul 13620, Republic of Korea

[9]SKKU Advanced Institute of Nanotechnology (SAINT), Sungkyunkwan University (SKKU), Suwon 16419, Republic of Korea

[10]These authors contributed equally

[11]Lead contact

*Correspondence: kimsw1@skku.edu (S.-W.K.), chonh@snu.ac.kr (N.-H.C.), bochoi@skku.edu (B.-O.C.)

https://doi.org/10.1016/j.xcrp.2022.100813

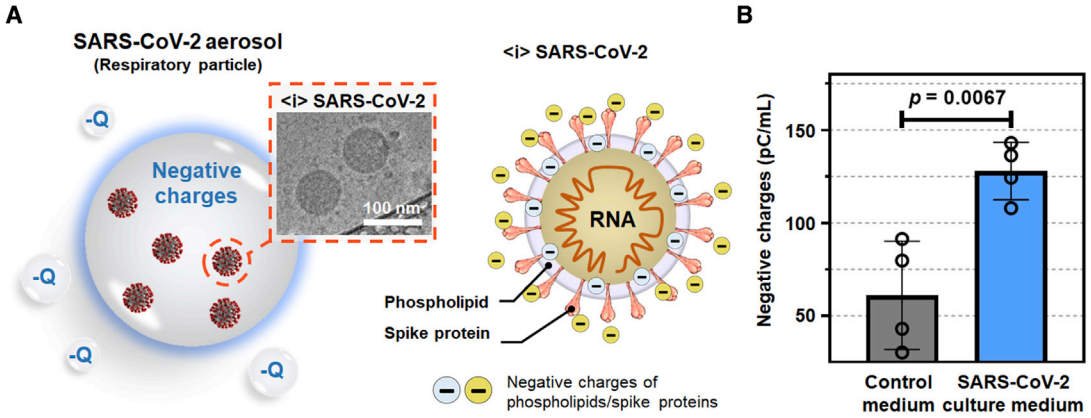

Figure 1. Negative charges of SARS-CoV-2

(A) Illustration of negatively charged SARS-CoV-2 and respiratory particles (inset figure: cryo-transmission electron microscopy image of SARS-CoV-2).
(B) Measured negative charges of SARS-CoV-2 culture medium and control medium. Data are from quadruplicated experiments and show the mean with error bars indicating SEM.

capture respiratory droplets by mechanical filtering. However, the filtration efficiency is reduced when the flow rate is high or the diameter of particles is small. In addition, mechanical filtering for sub-micrometer-size particles causes low breathability and high pressure drop because of the dense structure of the filter. Especially, there is a concern about contact transmission by contaminated filters since captured SARS-CoV-2 can survive on the surface of filters for several hours.[17–19]

Electrostatic interactions are thought to be involved in initiating virion assembly and receptor recognition of virions. Even though the surface charge of viral particles can be various, depending on viral composition and ionic environment in aqueous solution, most viral particles have negative net charges because they have isoelectric points below 7 at neutral pH.[20] In addition, enveloped viruses, including SARS-CoV-2, generally contain negatively charged phospholipids derived from host cells. However, experimental measurement of electrical charges is required since there are still multiple patches of positive and negative charges due to the large size of viral particles and their large variety of surface proteins.[21] Assuming the virus and respiratory particles have certain net charges, it can be inferred that repulsing respiratory particles by applying electric field (repulsive Coulomb force) is available to highly prevent the transmission of the virus. Especially, blocking respiratory particles through repulsion can be a novel mitigation technology because approaching viruses are preemptively blocked before they reach the filter, so it eliminates the possibility of contact infection by contamination. However, so far, there has been no experimental investigation on the electrical charges of SARS-CoV-2 and respiratory particles;[21,22] moreover, the concept of virus repulsion using Coulomb force has not been proposed.

RESULTS

Negative charges of SARS-CoV-2

Here, we propose a virus-blocking textile (VBT) that repulses SARS-CoV-2 respiratory particles using repulsive Coulomb force, powered by the human body's triboelectric energy harvesting. To confirm feasibility, we measured the electric charges of SARS-CoV-2 culture medium and control medium using a Faraday cup and electrometer.[23,24] The pH of media tested was 7.4, similar to the pH of respiratory droplets. SARS-CoV-2 aerosol has negative charges potentially due to negative charges of spike proteins and viral envelope composed of a phospholipids membrane in virus particles (Figure 1A; see Figure S1 for original cryo-transmission

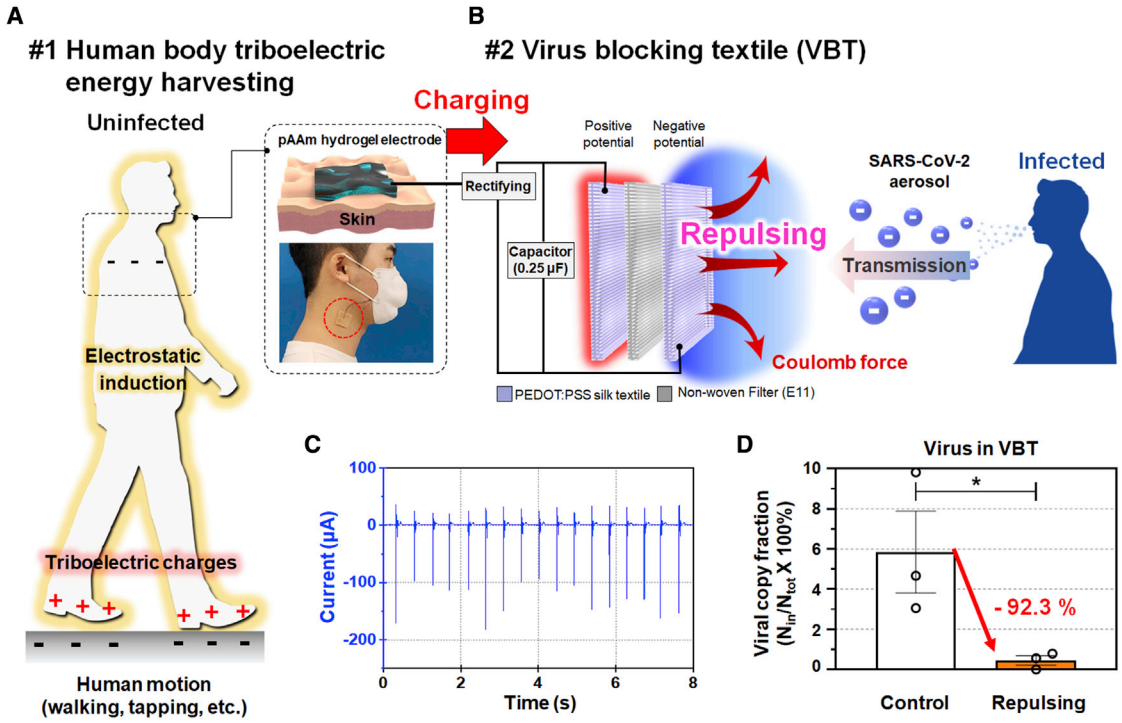

Figure 2. Concept and design of VBT for SARS-CoV-2

(A) Working principle of human body triboelectric energy harvesting to charge VBT.

(B) Concept of VBT that repulses SARS-CoV-2 aerosols using Coulomb force.

(C) An output current at 1-megohm impedance by hand tapping on PTFE.

(D) 13-fold (–92.3%) reduced viral copy fraction in VBT with potential of 180 V at flow rate of 0.5 m/s by repulsing SARS-CoV-2 aerosol in acrylic chamber study. The data show the mean with error bars indicating SEM (*p = 0.02).

electron microscopy image of SARS-CoV-2).[21,22] As shown in Figures 1B and S2, we found that SARS-CoV-2 culture medium has significantly greater negative charges (127.9 pC/mL) than control medium (61.1 pC/mL) ($t(6) = 4.06$, $p = 0.0067$, $d = 3.56$).

Concept of VBT using human body triboelectric energy harvesting

Continuously blocking SARS-CoV-2 respiratory particles can be achieved by the combination of (1) human body triboelectric energy harvesting and (2) VBT (Figure 2). (1) Human body triboelectric energy harvesting (Figure 2A): we charge VBT using human body triboelectric energy harvesting; then, the VBT has electrical potential. The human body can generate triboelectric charges by comprehensive human motions that make contact and separation with surrounding materials such as hand tapping, foot tapping (walking), and fluttering of clothing. Also, those triboelectric charges derive electrostatic induction of the human body, which has capacitive property. When we put an electrode to any skin, opposite charges are induced to the electrode, and AC current is generated to compensate the potential difference. Through rectifying the current, we can charge a VBT and a parallelly connected capacitor. (2) Virus-blocking textile (Figure 2B): the VBT is designed as a textile capacitor of a sandwich structure that consists of two conductive PEDOT:PSS coated silk textiles[25,26] and an insulating non-woven filter (Figure 2; see Figures S3 and S4 for detailed fabrication process). By charging the VBT using human body triboelectric energy harvesting, the foreside of the PEDOT:PSS silk textile of the VBT has negative electrical potential, so SARS-CoV-2 aerosol with negative charges is repulsed by repulsive Coulomb force.

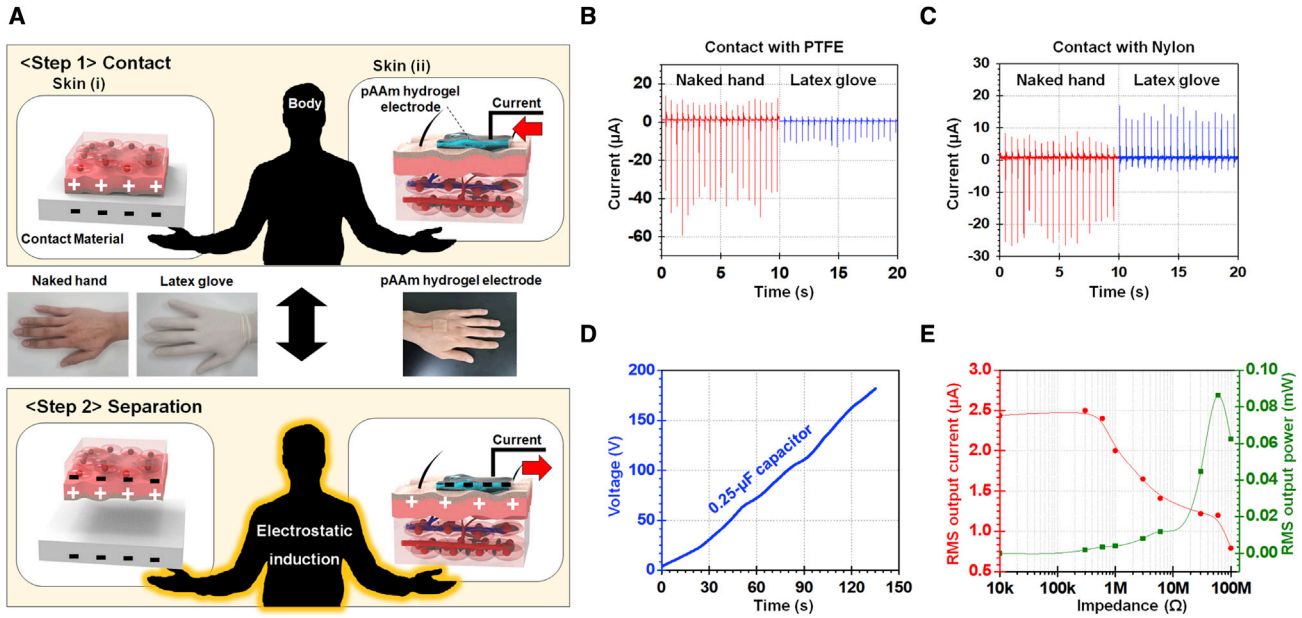

Figure 3. Working principle and electrical characterization of triboelectric output from the human body

(A) Diagram of the working principle of human body triboelectric energy harvesting. Inset figure: optical images of hands (skin (i), skin (ii)).

(B and C) An output current at 1-megohm impedance by hand tapping on (B) PTFE and (C) nylon without and with a latex glove.

(D) Charging curve of 0.25-μF capacitor by foot tapping on PTFE using a bridge rectifier.

(E) RMS output current at 1-megohm impedance and RMS output power depending on the electrical impedance by hand tapping on the PTFE.

We found that the human body can generate high output current reaching 212.9 μA (peak to peak) at most (Figure 2C). Considering that most kinds of human motion can generate high output current, human body triboelectric energy harvesting can be a sustainable and promising power source for VBTs. Detailed descriptions and characterizations for human body triboelectric energy harvesting are in Figure 3. Further, an acrylic chamber study that mimics respiratory contact shows that viral copy fraction in VBT (defined as the percentile fraction of viral RNA copies in VBT over total viral RNA copies in acrylic chamber) is 13-fold reduced (–92.3%) at a flow rate of 0.5 m/s when charging potential is 180 V. Detailed results are described in Figure 4.

Human body triboelectric energy harvesting

For an in-depth understanding of human body triboelectric energy harvesting, we demonstrate the working principle and output characteristics (Figure 3). The human body can generate output current when skin (i) repeatedly contacts and separates from contact materials, and a flexible and transparent polyacrylamide (pAAm) hydrogel electrode is on the skin (ii) (see experimental procedures for the fabrication process of pAAm hydrogel electrode).[27] In step 1, skin (i) has triboelectric charges by triboelectrification.[28] As it is separated in step 2, the human body is polarized by electrostatic induction. At this moment, to compensate electric potential difference, opposite charges are induced to the pAAm hydrogel electrode on the skin (ii), and current flows along to the external load. Reversely, when skin (i) contacts again, the electric potential difference in the human body is eliminated, and current flows in the opposite direction. In summary, human body triboelectric energy harvesting is enabled by the highly positive triboelectric characteristic and electric capacitive property of the human body.[29,30] An equivalent circuit model explaining the principles and theoretical calculation of output are described in Figure S5 and Note S1.

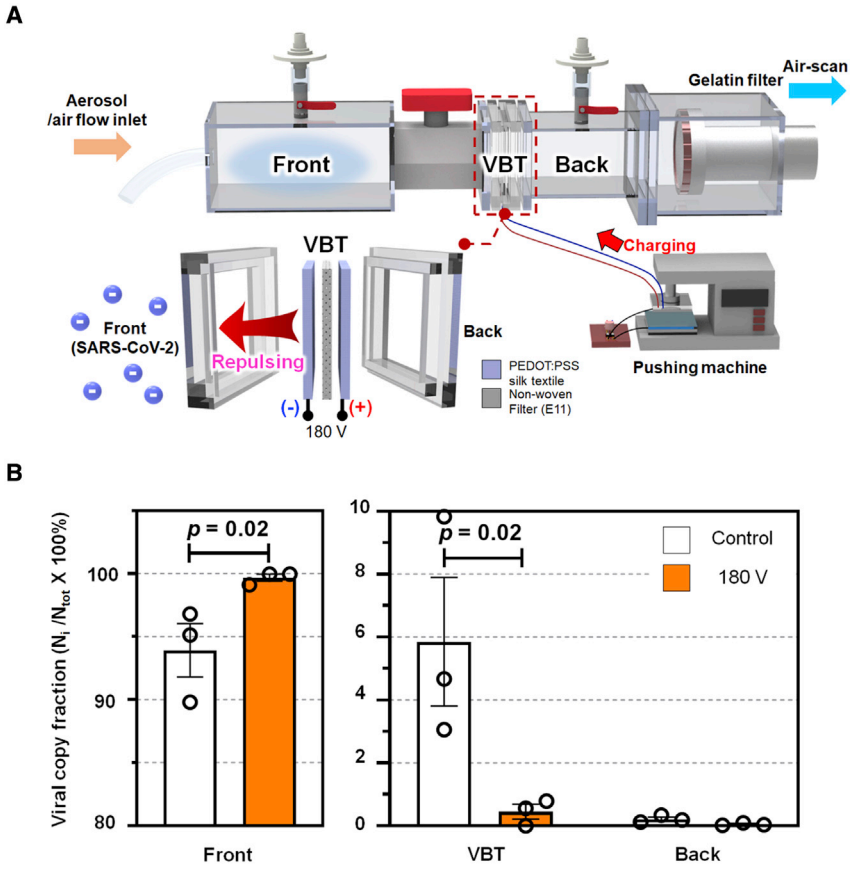

Figure 4. Blocking performance of VBT for SARS-CoV-2

(A) Experimental setup for acrylic chamber study.

(B) Changes in viral copy fractions of SARS-CoV-2 in each location when the potential of VBT is 0 V (control) and 180 V (test group) showing that VBT blocks 99.95% of SARS-CoV-2 by repulsing SARS-CoV-2 aerosols. Data are from triplicated experiments and show the mean with error bars indicating SEM.

We found that the human body generates high output current regardless of whether skin (i) is covered by dielectric material or not (latex glove in this study). Also, the level of output current depends on the quantity of triboelectric charges, which is determined by the kind of contacting material according to the triboelectric series. In this study, polytetrafluoroethylene (PTFE) and nylon 6,6 (Nylon) films were used as contact materials for electrical characterization since they are representative negative and positive triboelectric materials, respectively. When a hand without or with a latex glove contacts PTFE, the human body generates a peak-to-peak output current of 70.3 and 15.6 μA, respectively (Figure 3B, noted as naked hand and latex glove). When a hand without or with latex glove contacts nylon, the human body generates peak-to-peak output current of 35.0 and 20.2 μA, respectively (Figure 3C). Similarly, foot tapping on nylon with socks generates 83.8-μA peak-to-peak output current at most, and even a fluttering of clothing on the human body generates 3.0-μA peak-to-peak output current (Figure S6). Besides, the output current can be increased by strong tapping since large contacting force increases effective contact area and the quantity of triboelectric charges (Figure S7). The peak-to-peak output current reaches at most 259.6 μA by strong hand tapping on PTFE (Figure S8). In addition, the output current can be varied by changes in height, weight, and composition of bodies. Figure S9 shows triboelectric output current signals from three

different people, and peak-to-peak output current was still high, ranging from 150.5 to 212.9 μA.

It is noteworthy that triboelectric output current is generated regardless of where the electrode is, where contact occurs, or whether another material such as gloves or socks covers the skin. It means that we can harvest mechanical energy of most kinds of human motions that make contact. To confirm the self-powering performance, we demonstrate a charging curve of 0.25-μF capacitor using rectified output current by hand tapping on PTFE, and the potential of 0.25-μF capacitor quickly reaches 180 V in 134 s (Figure 3D). In addition, we measured root-mean-square (RMS) output current and RMS output power by hand tapping on PTFE at different electrical impedance (Figures 2E and S10). The human body generated 2.5-μA RMS output current at 1-megohm impedance and 0.09-mW RMS output power at optimum electrical impedance of 60 megohms. To highlight performance, we illuminate five commercial green light-emitting diodes using rectified output current (Video S1).

Virus blocking for SARS-CoV-2 using repulsive Coulomb force

To evaluate the blocking performance of VBT for SARS-CoV-2, we investigated the differences in viral copies in three locations (front chamber [Front], VBT, and back chamber [Back]) of an acrylic chamber after introducing SARS-CoV-2 aerosol to mimic the respiratory contact (Figures 4A and S11). Viral copy fraction is defined as the percentile fraction of viral RNA copies in each location over total viral RNA copies in the acrylic chamber. Viral aerosols of 3 μm diameter were generated by the nebulizer and introduced into the acrylic chamber, and additional air was injected at 0.5 m/s to mimic exhalation.[31] We charged the VBT and parallel-connected 0.25-μF capacitor to 180 V using rectified triboelectric output current by contact and separation between aluminum and polyfluoroalkoxy (PFA) film to mimic triboelectric output from the human body (Figure S12). The VBT was mounted between Front and Back for the foreside of the VBT to have negative potential. After respiratory contact demonstration, the mean viral copy fraction in the front chamber, VBT, and back chamber of the test group was 99.5%, 0.45%, and 0.05%, respectively (Figure 4B). Compared with the control group, viral copy fraction in the VBT was significantly decreased (13-fold; $t(12) = 3.16$, $p = 0.02$, $d = 2.15$), whereas that in the front chamber was significantly increased (1.06-fold; $t(12) = 3.37$, $p = 0.02$, $d = 2.05$), demonstrating that the viral aerosols were repelled from the VBT and pushed backward to the front chamber ($n = 3$). The viral copy fraction in back chamber was not significantly altered ($t(12) = 0.10$, $p = 0.93$, $d = 1.93$). As a result, we found that VBT highly blocks 99.95% of SARS-CoV-2 by repulsing the SARS-CoV-2 aerosols.

DISCUSSION

We showed here that 99.95% of SARS-CoV-2 was blocked by repulsion from the electrically charged VBT. It suggests that negatively charged SARS-CoV-2 aerosol particles cannot readily pass through VBT and hardly remain on the surface of the VBT, effectively preventing possible viral transmission. Moreover, it is noteworthy that VBTs can be constantly charged to high potential in a very short time by human body triboelectric energy harvesting and can efficiently block viral transmission, as shown in Figure 3D. Furthermore, it can be possibly applied for general enveloped viruses in considering that most enveloped viruses are known to have electric charges. Therefore, this study demonstrates a novel technology that provides effective, immediate mitigation of spread for not only SARS-CoV-2, but also variants and future emergent viruses before achieving population immunity using vaccines.

Furthermore, VBT has practical advantages to be applied to filters or face masks due to its high breathability, washability, and mechanical durability. In Figure S13, VBT shows 30.0% lower pressure drop of 72 Pa at 0.5 m/s of airflow than a commercial face mask (KF 94, 103 Pa), demonstrating high breathability of the VBT. This is because PEDOT:PSS silk textile has low fiber density (12 fibers in 1 mm). In Figure S14, PEDOT:PSS silk textile shows stable sheet resistance ranging from 2.0 kilohm/sq to 2.7 kilohm/sq, increased 35% during hand washing four times using neutral detergent. Scanning electron microscopy (SEM) images of PEDOT:PSS silk textile in Figure S15 show that there is no significant damage in the structure of textile and fibers after washing cycles. Also, we found that resistance of PEDOT:PSS silk textile only increases 13% after 10,000 stretch-release cycles with a strain of 10% (Figure S16). High washability and durability of PEDOT:PSS silk textile originates from PEDOT:PSS binding to silk fiber, forming a core-shell structure by electrostatic interactions,[25] and silk has intrinsic mechanical durability.

In conclusion, we developed an effective method to block SARS-CoV-2 using repulsive Coulomb force by incorporating human body triboelectric energy harvesting and conductive PEDOT:PSS silk textile. We found that the human body can be a high-performing power source that is enough to constantly charge VBT based on triboelectrification and electrostatic induction of the human body. Through evaluation using an acrylic chamber, it is found that VBT can effectively repulse SARS-CoV-2 aerosols, resulting in 99.95% of SARS-CoV-2 blocked. Finally, high breathability, washability, and durability of VBT were demonstrated, and this suggests that practical application of VBT as an effective face mask or filter is enabled.

EXPERIMENTAL PROCEDURES

Resource availability

Lead contact

The lead contact for this paper is Sang-Woo Kim (kimsw1@skku.edu).

Materials availability

This study did not generate new unique reagents.

Data and code availability

All of data supporting this study have been shown in the article and supplemental information. All other data are available from the lead contact upon reasonable request.

Fabrication of experimental samples

The VBT was composed of two conductive PEDOT:PSS silk textiles and an insulating non-woven filter (prefilter, filter class: E11). It had a sandwich structure for capacitance. The PEDOT:PSS silk textile was prepared by dyeing process as shown in Figure S3.[25,26] We purchased a commercial satin silk textile that has 12 fibers per millimeter. After gently dipping the commercial silk textile in PEDOT:PSS aqueous dispersion (1/2.5 ratio by weight) from Heraeus Epurio, it was annealed at 80°C for 30 min in an oven. To enhance electrical conductivity, the same process was repeated using methanol instead of PEDOT:PSS aqueous dispersion. Prepared PEDOT:PSS silk textiles and non-woven filter (E11) were cut into square pieces of size 5 cm, then the VBT was prepared by arranging and fixing pieces together using a commercial polyimide tape at the edges.

pAAm hydrogel electrode was prepared by sol-gel method and UV curing.[27] 2.5 g acrylamide, 3 mg N,N′-methylenebis (acrylamide), and 25 mg ammonium persulfate

were dissolved in 20 mL deionized water. After pouring the solution into the Petri dish mold, 20 μL N,N,N′,N′- tetramethyl ethylenediamine was added, and then the solution was cured by exposure of 365-nm UV light for 10 min, and the cured pAAm hydrogel was cut into squares of 3 cm dimension. All the aforementioned chemicals were purchased from Merck & Co.

We employed triboelectric output current that was generated by contact and separation between PFA film and aluminum to mimic human body triboelectric energy harvesting. After attaching aluminum tape to two acrylic substrates, a PFA film was attached to one of them using a carbon tape to enable contact and separation using a pushing machine (ATsolution SPG-01).

Electrical characterization

Voltage signals were measured using an oscilloscope (Tektronix DPO3052) using a probe (Tektronix P5100A) with 10-megohm input impedance. The current signals were measured using a low-noise current amplifier (FEMTO DLPCA-200) with 1-megohm input impedance, which was connected to the oscilloscope. A pushing tester (Z-tech ZPS-100) was used to impose consistently repeated contact and separation in electrical characterizations of triboelectric output current by PFA. The potential of the capacitors and VBT was measured using an electrometer (Keithley 6514). Electrical charges of SARS-CoV-2 culture medium and control media were measured using a handmade Faraday cup that was connected to the electrometer. The sheet resistance of PEDOT:PSS silk textiles was measured using a four-point probe.

Experimental setup for validation of virus blocking

VBT, pushing machine, bridge rectifier, and four serially connected 1-μF capacitors (0.25-μF capacitor) were connected to sustain the VBT potential, as shown in Figures S9 and S10. An acrylic chamber consisting of acrylic plates and several plumbing accessories was assembled to mimic respiratory contact. Nebulizer (Omron healthcare, Korea, NE-C28), front chamber, a valve, a VBT mount, and back chamber were serially connected by O-rings and anchors to form an air-tight structure. A gelatin filter (Sartorius Stedim, 17,528) to collect aerosols within the acrylic chamber was connected to an air sampler (Sartorius Stedim, MD8). A rotary pump (iNexus, Rocker300) was reversely connected in such a way to generate controlled unidirectional airflow in an acrylic chamber after introducing aerosols (Figure S11). A VBT mount was made up of two panels with square holes made at the center, where the VBT was loaded and exposed to aerosol flow. Two electric wires from each PEDOT:PSS silk textile were connected to the aforementioned circuit and aluminum electrodes for triboelectric output current generation by PFA film, which was mounted on a pushing machine (ATsolution, SPG-01).

Validation of virus blocking

For quantitative evaluation, the VBT and capacitors were powered by triboelectric output using a PFA film, and the potential was sustained at 0 V (control group) or 180 V (test group) while monitoring using an electrometer. The inflow of aerosol and flow rate was controlled by opening and closing three valves in the plumbing line and a valve between the front chamber and VBT mount. At first, viral aerosol (5.13×10^7 copies) was introduced into and filled the front chamber using a nebulizer with valves that closed other areas. Controlled airflow of 0.5 m/s or 2.5 m/s was run for 10 s to mimic breath and sneezing environments, respectively, using a rotary pump after closing the nebulizer valve and opening the valve between the front chamber and VBT mount. Then, after closing all valves, the virus in the back

chamber was first collected using an air sampler (50 L/min). After the tested VBT was separated, the VBT mount and a new gelatin filter were reassembled to collect virus particles left in the front chamber. Viral particles collected in the gelatin filters were dissolved in 4 mL PBS. The VBT was also suspended in PBS for viral RNA copy number quantification or in 4% paraformaldehyde for SEM imaging.

Virus isolation and RT-PCR

Viral RNA was isolated from the gelatin filter solution, VBT suspension, and culture medium using TRIzol-chloroform method as previously described. Briefly, the viral solutions were lysed with TRIzol LS (Life Technologies), and the RNA phase was isolated with chloroform and pelleted with an equal volume of isopropanol. The RNA pellet was washed with 75% ethanol twice and resuspended in DEPC-water. Extracted viral RNA was reverse transcribed with HiSenScript RH (–) RT Premix kit (Intron) according to the manufacturer's instructions. Quantitative RT-PCR was carried out on the cDNA formed with SensiFAST Probe Lo-ROX kit (Meridian Bioscience) as described by the manufacturer. Viral RNA copy number was quantified with standard curves and primer sets targeting RdRP genes of SARS-CoV-2.

Virus culture and preparation

SARS-CoV-2 isolate (South Korea, 2020) derived from a PCR-positive patient was kindly provided from Korea National Institute of Health. The SARS-CoV-2 isolate was propagated in Vero E6 cells for seven passages at low infection multiplicity for cell adaptation until the working stock solution was obtained. When generating virus aerosol with a nebulizer, 38.3% of fetal bovine serum was added to the virus solution to minimize the adhesion of viral particles to the wall of the acrylic chamber.

Virus and material characterization

The representative structure of SARS-CoV-2 was imaged using Cryo-EM after γ-irradiation. Viruses captured on VBT were imaged with SEM after 4% paraformaldehyde fixation. To characterize the surface morphology of VBT, it was fixed between two slide glasses, and cross-view optical microscopy images were obtained. Also, each sheet was attached to a glass substrate and top-view optical microscopy images were obtained. Data were analyzed using Prism 8 software (GraphPad). Statistical significance between groups was determined by unpaired Student's t test (two-tailed). Normal distribution was tested with Shapiro-Wilk test and Kolmogorov-Smirnov test. Estimates of effect sizes were calculated with Cohen's d.

To compare pressure drop by VBT and commercial mask (KF94), we mounted them with the dimension of 3.5 × 3.5 cm in the acrylic chamber. Airflow rates were set to 0.5 m/s using compressed gas, and the pressure drop was monitored in real time using the integrated sensors in the acrylic chamber. To evaluate washability and durability, PEDOT:PSS silk textiles were washed gently using commercial neutral detergent and dried for 6 h in ambient condition. Sheet resistance of PEDOT:PSS silk textile was measured using a four-point probe workstation (Chang Min, CMT-SR2000N). Surface morphology and fiber structure of PEDOT:PSS silk textile were examined by scanning electron microscopy (Jeol, JSM-6701F, FE-SEM). We repeatedly elongated PEDOT:PSS silk textile using a bending tester (Z-TEC, ZBT-200) and resistance was measured using a multimeter (Donghwa electronics, DM-1010).

SUPPLEMENTAL INFORMATION

Supplemental information can be found online at https://doi.org/10.1016/j.xcrp.2022.100813.

ACKNOWLEDGMENTS

This work was financially supported by the Nano Material Technology Development Program (2020M3H4A1A03084600), the Basic Science Research Program (2021R1A2C2010990), and the Bio & Medical Technology Development Program (2021M3A9I2080490) through the National Research Foundation of Korea (NRF) funded by Ministry of Science and ICT.

AUTHOR CONTRIBUTIONS

S.-W.K., M.K., J.-H.A., H.M.K., and B.-O.C. designed and conceptualized the project. M.K. and H.T.K. conducted early stage of characterization of triboelectric output from the human body. M.K. and Y.-J.K. designed and fabricated experimental setup for the blocking performance evaluation of VBT. N.-H.C. supervised all experiments using the virus. Y.K. designed the early setup of the acrylic chamber to evaluate blocking performance of VBT. N.-Y.J. and H.-J.R. prepared SARS-CoV-2 and conducted electrical characterization of SARS-CoV-2 and blocking performance evaluation of VBT. D.K. fabricated VBT samples. All authors wrote the manuscript.

DECLARATION OF INTERESTS

The authors declare no competing interests.

Received: July 17, 2021
Revised: January 10, 2022
Accepted: February 23, 2022
Published: March 15, 2022

REFERENCES

1. Vallamkondu, J., John, A., Wani, W.Y., Ramadevi, S.P., Jella, K.K., Reddy, P.H., and Kandimalla, R. (2020). SARS-CoV-2 pathophysiology and assessment of coronaviruses in CNS diseases with a focus on therapeutic targets. Biochim. Biophys. Acta Mol. Basis. Dis. *1866*, 165889.

2. Sohrabi, C., Alsafi, Z., O'Neill, N., Khan, M., Kerwan, A., Al-Jabir, A., Iosifidis, C., and Agha, R. (2020). World Health Organization declares global emergency: a review of the 2019 novel coronavirus (COVID-19). Int. J. Surg. *76*, 71–76.

3. Fontanet, A., Autran, B., Lina, B., Kieny, M.P., Karim, S.S.A., and Sridhar, D. (2021). SARS-CoV-2 variants and ending the COVID-19 pandemic. Lancet *397*, 952–954.

4. Das, P., Satter, S.M., Ross, A.G., Abdullah, Z., Nazneen, A., Sultana, R., Rimi, N.A., Chowdhury, K., Alam, R., Parveen, S., et al. (2021). A case series describing the recurrence of COVID-19 in patients who recovered from initial illness in Bangladesh. Trop. Med. Infect. Dis. *6*, 41.

5. Chen, R.E., Zhang, X., Case, J.B., Winkler, E.S., Liu, Y., VanBlargan, L.A., Liu, J., Errico, J.M., Xie, X., Suryadevara, N., et al. (2021). Resistance of SARS-CoV-2 variants to neutralization by monoclonal and serum-derived polyclonal antibodies. Nat. Med. *27*, 717–726.

6. Hoffmann, M., Arora, P., Groß, R., Seidel, A., Hörnich, B.F., Hahn, A.S., Krüger, N., Graichen, L., Hofmann-Winkler, H., Kempf, A., et al. (2021). SARS-CoV-2 variants B.1.351 and P.1 escape from neutralizing antibodies. Cell *184*, 2384–2393.

7. Hassan, I., Mukaigawara, M., King, L., Fernandes, G., and Sridhar, D. (2021). Hindsight is 2020? lessons in global health governance one year into the pandemic. Nat. Med. *27*, 396–400.

8. Kim, J.H., Marks, F., and Clemens, J.D. (2021). Looking beyond COVID-19 vaccine phase 3 trials. Nat. Med. *27*, 205–211.

9. Anderson, R.M., Heesterbeek, H., Klinkenberg, D., and Hollingsworth, T.D. (2020). How will country-based mitigation measures influence the course of the COVID-19 epidemic? Lancet *395*, 931–934.

10. Shiu, E.Y.C., Leung, N.H.L., and Cowling, B.J. (2019). Controversy around airborne versus droplet transmission of respiratory viruses: implication for infection prevention. Curr. Opin. Infect. Dis. *32*, 372–379.

11. Tellier, R., Li, Y., Cowling, B.J., and Tang, J.W. (2019). Recognition of aerosol transmission of infectious agents: a commentary. BMC Infect. Dis. *19*, 101.

12. Cheng, Y., Ma, N., Witt, C., Rapp, S., Wild, P.S., Andreae, M.O., Pöschl, U., and Su, H. (2021). Facemask effectively limit the probability of SARS-Cov-2 transmission. Science *372*, 1439–1443.

13. Lindsley, W.G., Noti, J.D., Blachere, F.M., Szalajda, J.V., and Beezhold, D.H. (2014). Efficacy of face shields against cough aerosol droplets from a cough simulator. J. Occup. Environ. Hyg. *11*, 509–518.

14. Asadi, S., Cappa, C.D., Barreda, S., Wexler, A.S., Bouvier, N.M., and Ristenpart, W.D. (2020). Efficacy of masks and face coverings in controlling outward aerosol particle emission from expiratory activities. Sci. Rep. *10*, 15665.

15. Leung, N.H.L., Chu, D.K.W., Shiu, E.Y.C., Chan, K.-H., McDevitt, J.J., Hau, B.J.P., Yen, H.-L., Li, Y., Ip, D.K.M., Peiris, J.S.M., et al. (2020). Respiratory virus shedding in exhaled breath and efficacy of face masks. Nat. Med. *26*, 676–680.

16. Konda, A., Prakash, A., Moss, A.G., Schmoldt, M., Grant, G.D., and Guha, S. (2020). Aerosol filtration efficiency of common fabrics used in respiratory cloth masks. ACS Nano. *14*, 6339–6347.

17. Virtanen, J., Aaltonen, K., Kivistö, I., and Sironen, T. (2021). Survival of SARS-CoV-2 on clothing materials. Adv. Virol. *2021*, 6623409.

18. Liu, Y., Li, T., Deng, Y., Liu, S., Zhang, D., Li, H., Wang, X., Jia, L., Han, J., Bei, Z., et al. (2021). Stability of SARS-CoV-2 on environmental surfaces and in human excreta. J. Hosp. Infect. *107*, 105–107.

19. Greatorex, J.S., Digard, P., Curran, M.D., Moynihan, R., Wensley, H., Wreghitt, T., Varsani, H., Garcia, F., Enstone, J., and Nguyen-Van-Tam, J.S. (2011). Survival of *Influenza A*(H1N1) on materials found in

households: implications for infection control. PLoS One *6*, e27932.

20. Michen, B., and Graule, T. (2010). Isoelectric points of viruses. J. Appl. Microbiol. *109*, 388–397.

21. Joonaki, E., Hassanpouryouzband, A., Heldt, C.L., and Areo, O. (2020). Surface chemistry can unlock drivers of surface stability of SARS-CoV-2 in a variety of environmental conditions. Chem. *6*, 2135–2146.

22. Javidpour, L., Božič, A., Naji, A., and Podgornik, R. (2021). Electrostatic interactions between the SARS-CoV-2 virus and a charged electret fibre. Soft Matter *17*, 4296–4303.

23. Hunt, J.F., Fang, K., Malik, R., Snyder, A., Malhotra, N., Platts-Mills, T.A., and Gaston, B. (2000). Endogenous airway acidification. Implication for asthma pathophysiology. Am. J. Respir. Crit. Care Med. *161*, 694–699.

24. Cezan, S.D., Nalbant, A.A., Buyuktemiz, M., Dede, Y., Baytekin, H.T., and Baytekin, B. (2019). Control of triboelectric charges on common polymers by photoexcitation of organic dyes. Nat. Commun. *10*, 276.

25. Ryan, J.D., Mengistie, D.A., Gabrielsson, R., Lund, A., and Müller, C. (2017). Machine-washable PEDOT:PSS dyed silk yarns for electronic textiles. ACS App. Mater. Inter. *9*, 9045–9050.

26. Alemu, D., Wei, H.-Y., Ho, K.-C., and Chu, C.-W. (2012). Highly conductive PEDOT:PSS electrode by simple film treatment with methanol for ITO-free polymer solar cells. Energy Environ. Sci. *5*, 9662–9671.

27. Xiong, C., Wei, F., Li, W., Liu, P., Wu, Y., Dai, M., and Chen, J. (2018). Mechanism of polyacrylamide hydrogel instability on high-temperature conditions. ACS Omega *3*, 10716–10724.

28. Chen, J., Zhu, G., Yang, J., Jing, Q., Bai, P., Yang, W., Qi, X., Su, Y., and Wang, Z.L. (2015). Personalized keystroke dynamics for self-powered human-machine interfacing. ACS Nano. *9*, 105–116.

29. Tat, T., Libanori, A., Au, C., Yau, A., and Chen, J. (2021). Advances in triboelectric nanogenerators for biomedical sensing. Biosens. Bioelectron. *171*, 112714.

30. Zhao, J.F., Chen, X.M., Liang, B.D., and Chen, Q.X. (2017). A review on the human body communication: signal propagation model, communication performance, and experimental issues. Wirel. Commun. Mob. Comput. *2017*, 1–15.

31. Tang, J.W., Nicolle, A.D., Klettner, C.A., Pantelic, J., Wang, L., Suhaimi, A.B., Tan, A.Y.L., Ong, G.W.X., Su, R., Sekhar, C., et al. (2013). Airflow dynamics of human jets: sneezing and breathing - potential sources of infectious aerosols. PLoS One *8*, e59970.